Available online at www.sciencedirect.com
SCIENCE DIRECT®
Journal of the European Ceramic Society 25 (2005) 3027–3031
www.elsevier.com/locate/jeurceramsoc

Electrical properties of screen-printed $NiMn_2O_{4+\delta}$

R. Schmidt *, A.W. Brinkman

University of Durham, Department of Physics, South Road, Durham DH1 3LE, UK

Available online 5 April 2005

Abstract

The direct current (dc) resistance versus temperature (*R–T*) characteristics and the alternating current (ac) impedance of thick screen-printed films made of ceramic $NiMn_2O_{4+\delta}$ thermistor material have been analysed. Electron transport in spinel NTCR thermistors is commonly described by an Arrhenius hopping model ($R \sim T\exp(T_0/T)$) for nearest neighbour hopping (NNH) or by different variable range hopping (VRH) models ($R \sim T^{2p}\exp(T_0/T)^p$). In screen-printed films dc conduction was well described by VRH with $p \sim 0.5$, indicating that the shape of the density of states (DOS) was parabolic. Values of T_0 ranged from 1.90×10^5 K to 1.97×10^5 K. Impedance spectroscopy was carried out at a frequency range of 5 Hz–6 MHz between 60 °C and 220 °C. For frequencies below ~2.7 MHz the complex impedance was well described by a standard equivalent circuit, based on one parallel resistance–capacitance (*RC*) element. Plots on the complex plane of the imaginary versus real parts of the impedance (Z''–Z' loci) showed one regular semicircle at each temperature, from which the capacitance and resistance of the *RC* element were determined. The capacitance was found to be in the order of 1×10^{-12} F at all temperatures, indicating a grain effect. The ac resistance versus temperature characteristics were in very good agreement with the dc results and followed the same VRH model with $p \sim 0.5$. At frequencies above 2.7 MHz the impedance could not be described by a standard *RC* element.

Keywords: Films; Impedance; Spinels; Thermistors

1. Introduction

$NiMn_2O_{4+\delta}$ is a strongly correlated system, where the crystal structure and the electrical properties are closely linked.[1] The material has a typical cubic spinel structure based on an oxygen fcc sublattice, where, in the case of a regular spinel, the divalent cations are situated on tetrahedral and the trivalent cations on octahedral lattice interstices. $NiMn_2O_{4+\delta}$ is an intermediate type spinel where a fraction x of the Ni^{2+} cations are displaced from the tetrahedral to the octahedral sites. A corresponding proportion $2x$ of Mn^{3+} cations disproportionate to Mn^{2+} and Mn^{4+}, and the Mn^{2+} cations move to the tetrahedral sites to compensate Ni^{2+} vacancies.[2] Electron transport is based on thermally activated electron hopping between Mn^{3+} and Mn^{4+} and the resistivity exhibits an uniform exponential increase with decreasing temperature (NTCR) over a wide range of temperature (~150 K–450 K), which makes the compound well suited for use as a thermistor material in temperature sensing applications.

The material has been widely used in industry as a temperature sensor in bulk material, but in this form there are often problems with poor stability, reproducibility and pores. These difficulties can be minimised in polycrystalline films, which have been produced by screen-printing as described in a previous publication.[3] In this paper, the temperature dependent ac impedance characteristics of screen-printed films are compared to the dc resistance versus temperature (*R–T*) characteristics.

2. Electron hopping

Electrical conductivity in $NiMn_2O_{4+\delta}$ is dependent on the concentration of donor (Mn^{3+}) and acceptor (Mn^{4+}) electron states. Macroscopically, this is a percolation problem with a percolation threshold parameter ξ_C, that includes both spatial

* Corresponding author. Present address: Department of Materials Science and Metallurgy, University of Cambridge, Pembroke Street, Cambridge CB2 3QZ, UK. Tel.: +44 1223 334375; fax: +44 1223 334373.
E-mail address: rs441@cam.ac.uk (R. Schmidt).

0955-2219/$ – see front matter © 2005 Elsevier Ltd. All rights reserved.
doi:10.1016/j.jeurceramsoc.2005.03.180

and energy contributions[4]:

$$\xi_C \geq \frac{2r_{ij}}{a} + \frac{\varepsilon_{ij}}{k_B T} \quad (1)$$

where r_{ij} and ε_{ij} are the separation in real and energy space of the i and j electron states, respectively and a is a localisation length. The relative magnitudes of the two terms on the right hand side of expression (1) determine whether or not hopping is constrained to nearest neighbours, and evidently at sufficiently high temperatures it always is. The resistivity ρ is given in the general case by:

$$\rho = \rho_0 \exp(\xi_C) \quad (2)$$

where ρ_0 depends on particular physical and material properties of the system. In $NiMn_2O_{4+\delta}$ a small polaron is associated with the electron transfer due to the Jahn–Teller distortion of the unit cell originating from the Mn^{3+} cation and the resistivity is then given by[5]:

$$\rho = \frac{36k_B T\pi^3 D_V s^5 \hbar^4 \varepsilon_r^2 \varepsilon_0^2 a^4 \exp(\xi_C)}{e^6 n E_1^2 r_{ij}^4 \varepsilon_{ij}} \quad (3)$$

n is the Mn^{3+}concentration, E_1 the deformation energy of the donor site, D_V density, s the velocity of sound and $\varepsilon_r \times \varepsilon_0$ the permittivity of the material. Substitution of ξ_C, r_{ij} and ε_{ij} into expression (3) gives for variable-range hopping (VRH):

$$\rho(T) = CT^{2p} \exp\left(\frac{T_0}{T}\right)^p \quad (4)$$

where C comprises all constant parameters. The index p depends principally on the shape of the density of states (DOS): for a uniform DOS $p = 1/4$, while for a parabolic distribution of the DOS around the Fermi level, $p = 1/2$. In the latter case T_0 is given by[4]:

$$T_0 = \frac{\beta e^2}{4\pi\varepsilon_r\varepsilon_0 a k_B} \quad (5)$$

where the numerical constant $\beta = 3.99$ for polaron hopping.

3. ac impedance spectroscopy

The principles of ac impedance spectroscopy applied to polycrystalline ceramic materials have been described by Irvine et al.,[6] who used a brick layer model to discriminate and quantify grain, grain boundaries and electrode contributions to the overall impedance. This model assumes a simplified cubic shape of the grains separated by grain boundary areas, and that the components of the overall impedance due to grains, grain boundaries are qualitatively and quantitatively different. If the material is uniform with a sufficiently narrow grain size distribution, and grain, grain boundary and electrode behave consistently throughout the sample, then the macroscopic impedance can be interpreted as an average of the microscopic effects.[7] Each element may be represented by a single resistance–capacitance (RC) element and the equivalent circuit is just the series connection of all RC components. Individual R and C values can be obtained from the Z''–Z' loci, where ideally a perfect semicircle appears for each RC element. The dimensions of the semicircle allow the determination of R and C.

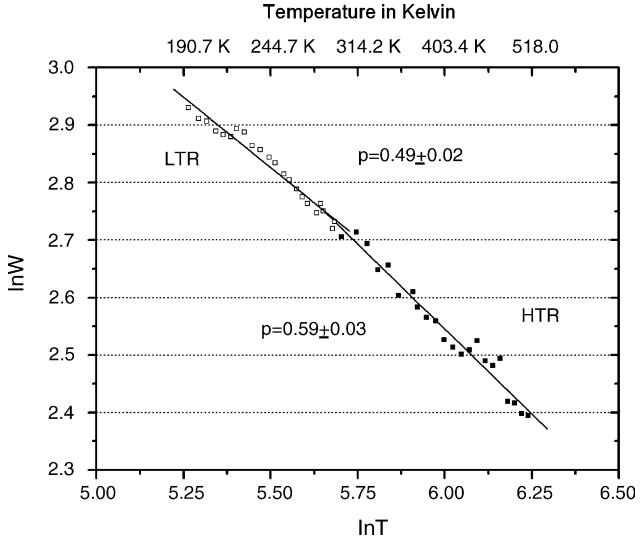

Fig. 1. ln(W) vs. ln(T) plots, film sintered at 850 °C for 30 min, HTR and LTR, dc measurements.

We have previously shown that in screen-printed layers the grain size distribution was uniform and narrow,[3] and the brick layer model was therefore assumed to be valid here.

4. Experimental methods

$NiMn_2O_{4+\delta}$ starting material for the screen printing was prepared by co-precipitation of mixed precursor oxalates and

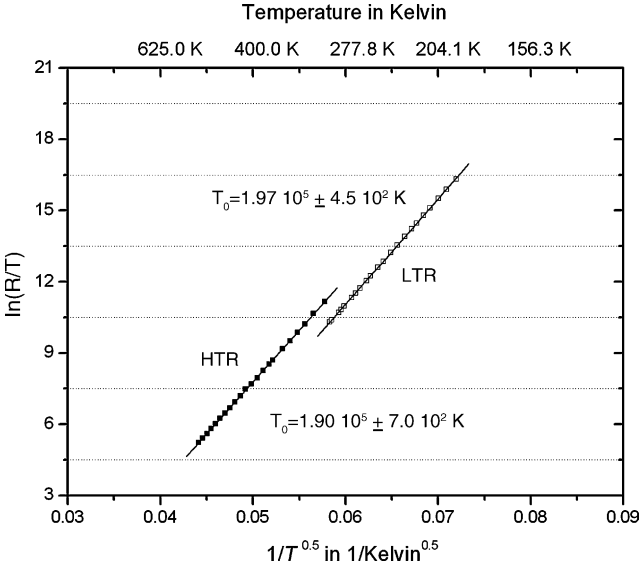

Fig. 2. ln(R/T) vs. $1/T^{0.5}$ plots, film sintered at 850 °C for 30 min, HTR and LTR, dc measurements.

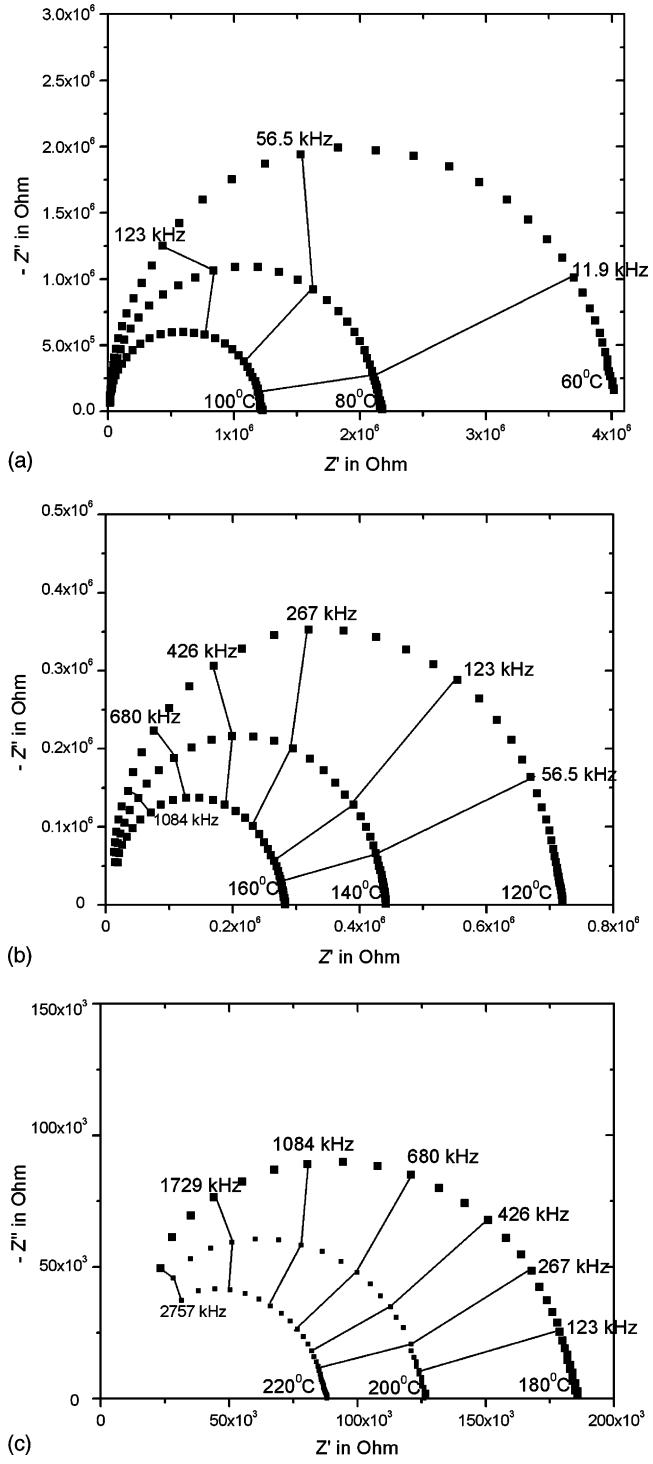

Fig. 3. (a) $-Z''$ vs. Z' complex plane locus, 60 °C–100 °C. (b) $-Z''$ vs. Z' complex plane locus, 120 °C–160 °C. (c) $-Z''$ vs. Z' complex plane locus, 180 °C–220 °C, ac measurements.

their subsequent firing. A glass phase, organic dispersing agent and common organic binder and solvents were added and thick films (∼20 μm) printed onto Al_2O_3 substrates followed by sintering for 30 min at 850 °C. Sample preparation methods and structural characterisation of the films have been described more fully elsewhere.[3]

Two circular Al contacts were evaporated onto the film surfaces and were covered with quick drying silver paint to prevent oxidation. Copper wires were attached with solder and the Ohmic behaviour of the contacts was confirmed. "Two point" dc measurements were performed with different systems. For high temperature regime (HTR) measurements

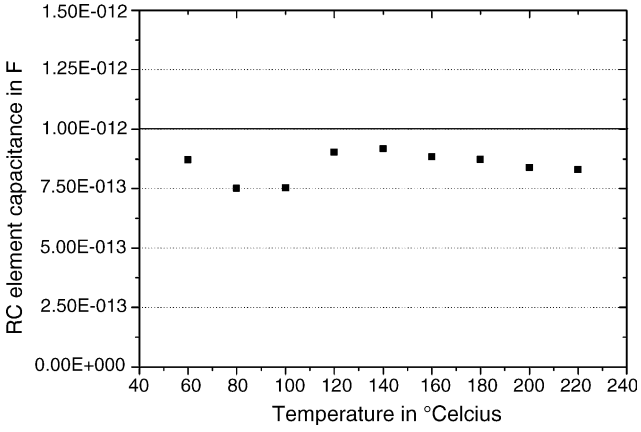

Fig. 4. *RC* element capacitance vs. temperature.

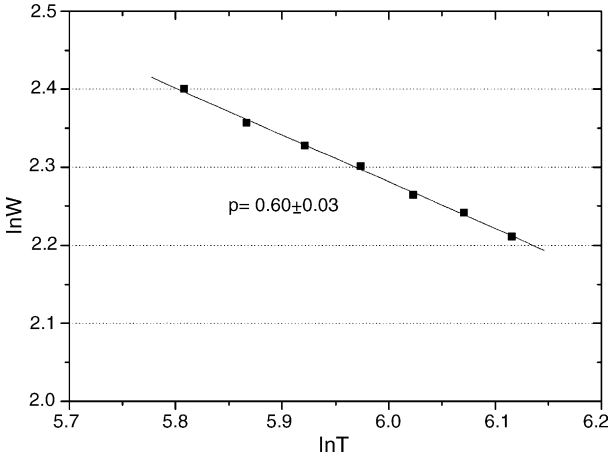

Fig. 5. ln(*W*) vs. ln(*T*) plot for ac data.

(300 K–530 K) the samples were placed in a purpose built insulated furnace equipped with a temperature controller linked to a thermocouple inside the furnace. Low temperature regime (LTR) characteristics (180 K–300 K) were measured in a standard cryostat connected to an electrometer and temperature controller. Data was recorded using an automated data acquisition system, which ensured complete temperature and resistance stability before taking *R–T* readings.

For ac impedance spectroscopy again two circular Al/Ag contacts were used and the samples placed in a PTFE purpose-built sample holder equipped with two spring loaded drop-down contacts, designed to minimise the electrode-sample interface effects.[8] Impedance spectroscopy was carried out in the HTR system over the temperature range of 60 °C–220 °C in 20 °C intervals. Impedance spectra were taken using a Hewlett/Packard 4192A LF Impedance Analyser with computer controlled automated data collection ("Integrated Impedance Analyser Programme", Version #2.6, 1991), which increased the frequency logarithmically between 5 Hz and 6 MHz. The alternating test signal (amplitude 3 V) was superimposed on a 30 V dc bias voltage in order to reduce noise. Parasitic contributions were eliminated by correcting the spectra against a previous open circuit calibration measurement.

5. Results

The dc and ac *R–T* data were analysed following the procedure described by Shklovskii and Efros,[4] in which the index parameter p in (4) is given by the slope of a plot of ln(W) versus ln(T) where

$$W = \frac{1}{T}\frac{\mathrm{d}(\ln \rho)}{\mathrm{d}(T^{-1})} \approx -p\left(\frac{T_0}{T}\right)^p \tag{6}$$

This is a powerful technique to elucidate the character of hopping motion.

For dc measurements the HTR and LTR plots of ln(W) versus ln(T) are given in Fig. 1 and show that $p \sim 0.5$, indicating that transport was by VRH with a parabolic distribution of the DOS. The corresponding *R–T* data was plotted as ln(R/T) versus $1/T^{0.5}$ in Fig. 2, appropriate for a VRH model with a parabolic DOS, and the T_0 values were determined from the slopes. Using Eq. (5), the product $\varepsilon_r \times a$ was calculated to be 3.18 Å–3.53 Å. Upper limits for the effective Bohr radii a, based on a hard sphere model, have been published by O'Neill and Navrotsky[9]: 0.72 Å and 0.67 Å for Mn^{3+} and Mn^{4+}, respectively, and imply that the lower limit of the dielectric constant should be $\varepsilon_r \geq 4.4$.

The ac impedance Z''–Z' loci are shown in Fig. 3a–c. Clearly one semicircle occurred at each temperature, but the loci were regular only below a frequency limit of ~2.7 MHz and have been plotted only in these regions. At higher frequencies the Z''–Z' loci were not consistent anymore with the behaviour expected for a *RC* element.

For the regular semicircles, the capacitance C and resistance R were calculated from the semicircle dimensions. The capacitance was found to be in the range of 1×10^{-12} F at all temperatures (see Fig. 4), which, according to Irvine et al.,[6] may be associated with a bulk grain effect.

The ac *R–T* characteristics were analysed in the same way as the dc, and the corresponding ln(W) versus ln(T) plot is shown in Fig. 5. Since $p \sim 0.5$, it is indicated that the conduction mechanism was VRH with a parabolic DOS, and the dc measurements agreed well with the ac data. The *R–T* data was again plotted as ln(R/T) versus $1/T^{0.5}$ and the slope of the graph lead to a characteristic temperature T_0 of 1.88×10^5 K, which is in excellent agreement with the dc value of 1.90×10^5 K.

6. Conclusions

It was concluded that conduction was uniform across the sample, because only one semicircle occurred in the Z''–Z' loci, and the corresponding *RC* element showed *R–T*

characteristics identical to the dc variable-range hopping model. The dc characteristics were simply the low frequency limit of the ac data, and gave a lower limit on the dielectric constant of $\varepsilon_r \geq 4.4$. The VRH model with $p \sim 0.5$ suggested that in $NiMn_2O_{4+\delta}$ the DOS may be of parabolic shape around the Fermi-level.

Generally, in terms of their applicability for use as thermistors, screen-printed films seem to offer significant advantages; conduction appears to be well controlled while the technology is suited to low cost volume production.

References

1. Tsuda, N., Nasu, K., Fujimori, A. and Siratori, K., Electronic conduction in oxides. In *Solid-State Sciences*, ed. M. Cardona, P. Fulde, K. von Klitzing, R. Merlin, H. J. Queisser and H. Störmer. Springer, Berlin, 2000.
2. Macklen, E. D., *Thermistors*. Electrochemical Publications, Glasgow, 1979.
3. Schmidt, R., Stiegelschmitt, A., Roosen, A. and Brinkman, A. W., Screen printing of coprecipitated $NiMn_2O_4$ for production of NTC thermistors. *J. Eur. Ceram. Soc.*, 2003, **23**(10), 1549–1558.
4. Shklovskii, B. I. and Efros, A. L., Electronic properties of doped semiconductors. In *Solid State Sciences, Vol 45*. Springer-Verlag, Berlin, 1984.
5. Tuller, H. L. and Nowick, A. S., Small polaron electron transport in reduced CeO_2 single crystals. *J. Phys. Chem. Solids*, 1977, **38**, 859.
6. Irvine, J. T. S., Sinclair, D. C. and West, A. R., Electroceramics: characterization by impedance spectroscopy. *Adv. Mater.*, 1990, **2**(3), 132.
7. Fleig, J. and Mayer, J., The impedance of ceramics with highly resistive grain boundaries: validity and limits of the brick layer model. *J. Eur. Ceram. Soc.*, 1999, **19**, 693.
8. Hwang, J.-H., Kirkpatrick, K. S., Mason, T. O. and Garboczi, E. J., Experimental limitations in impedance spectroscopy: part IV. Electrode contact effects. *Solid State Ionics*, 1997, **98**, 93.
9. O'Neill, H. S. C. and Navrotsky, A., Simple spinels: crystallographic parameters, cation radii, lattice energies, and cation distribution. *Am. Mineral.*, 1983, **68**, 181.